

Introduction to Strong Alfvénic MHD Turbulence

Jungyeon Cho

Department of Astronomy and Space Science, Chungnam National University, 99 Daehak-ro, Daejeon, 34134, Korea (ROK).

Contributing authors: jcho@cnu.ac.kr;

Abstract

Many astrophysical fluids are magnetized and turbulent. Such fluids can be often described by magnetohydrodynamics (MHD). In this review, we mainly consider MHD turbulence with a strong mean magnetic field whose energy density is greater than or equal to the local kinetic energy density. In these fluids, the MHD waves, especially Alfvén waves, play a dominant dynamical role. Alfvén waves travel along magnetic field lines and collisions of opposite-traveling Alfvén wave packets are essential for turbulence cascade. We focus on strong turbulence regime, where nonlinear interaction during the collision is sufficiently strong and thus one collision is enough to complete turbulence cascade. We will cover the following types of turbulence. First, we review strong Alfvénic MHD turbulence. If the mean magnetic field is very strong, wave packets move very fast and duration of collision is too short to complete turbulence cascade. Even in this case we will show that strong turbulence regime emerges on a small scale. Second, we will consider small-scale MHD turbulence, where interaction of small-scale variants of Alfvén waves (i.e., whistler waves) is important. Third, we review scaling relations in strong relativistic force-free MHD turbulence, where interaction of relativistic Alfvén waves is important. Finally, we briefly discuss scaling relations in compressible MHD turbulence, where interaction of Alfvén waves is still important.

Keywords: turbulence, magnetic field, magnetohydrodynamics, Alfvén wave

1 Introduction

Since astrophysical fluids exhibit turbulent motions and magnetic fields are undoubtedly found in such fluids, magnetohydrodynamic (MHD) turbulence is an important field of study in astronomy. In most astrophysical plasmas, the magnetic Reynolds

number easily exceeds 10^{10} . In such a system, the usual expectation is that magnetic field is frozen into the fluid. The velocity field advects and stretches magnetic field lines and magnetic field exerts pressure and tension forces on velocity field. Therefore, MHD turbulence is different from pure hydrodynamic turbulence.

Consider incompressible MHD turbulence in a system threaded by a uniform external (or ‘mean’) magnetic field. Then we may consider two extreme cases: strong mean field cases and weak/zero mean field cases. Numerical studies show that zero mean field cases are virtually identical to weak mean field cases after turbulence reaches a statistically stationary state (see, for example, [Cho 2014](#)). Therefore we may put weak and zero mean field cases into the same category. When the mean field is weak/zero, turbulence motions can efficiently amplify magnetic field (see, for example, [Batchelor 1950](#); [Kazantsev 1968](#); [Meneguzzi et al. 1981](#); [Kida et al. 1991](#); [Cho and Vishniac 2000b](#); [Schekochihin et al. 2004](#); [Cho et al. 2009](#); [Brandenburg et al. 2012](#)). As a result of this turbulence dynamo process, magnetic energy density initially grows and, as magnetic field gets stronger, magnetic back reaction becomes important. When magnetic field becomes sufficiently strong, turbulence dynamo process saturates due to magnetic back reaction and growth of magnetic energy density stops. Numerical simulations ([Cho and Vishniac 2000b](#); [Cho et al. 2009](#)) show that, after turbulence reaches the saturation stage, coherence length of the magnetic field is comparable to the driving scale and that, below a scale slightly smaller than the energy injection scale, magnetic and kinetic energy densities are roughly in equipartition. This result implies that, even if the mean field is weak/zero, turbulence on small scales can be regarded as turbulence threaded by a strong mean field. In this paper, we focus on MHD turbulence threaded by a strong mean field.

When external mean magnetic field is strong, MHD waves play important roles. In incompressible fluids, there are two types of MHD waves: shear Alfvén and pseudo-Alfvén waves. They have the same dispersion relation and propagate along the magnetic field lines at the Alfvén speed, which is proportional to the strength of the magnetic field:

$$V_A = B_0 / \sqrt{4\pi\rho}, \quad (1)$$

where B_0 is the strength of the mean field and ρ is density¹. Detailed studies show that pseudo-Alfvén waves are only passively evolved by Alfvén waves ([Goldreich and Sridhar 1995, 1997](#)). In this sense, Alfvén waves play fundamental roles in magnetized plasmas: they determine dynamics of incompressible magnetized plasmas with a strong background field. Therefore, in this paper, we will focus on Alfvén waves. It is important to note that Alfvén waves are non-dispersive and thus Alfvén waves moving in one direction do not interact. Only counter-traveling Alfvén waves interact.

When two opposite-traveling Alfvén wave packets of similar sizes collide, nonlinear interactions will distort themselves and give rise to energy cascade to smaller scales. Then the question is the strength of the nonlinear interaction. If nonlinear interaction is sufficiently strong, then one collision can be enough to complete energy cascade.

¹In numerical simulations, it is customary to use a system of units in which 4π does not appear (i.e., $4\pi = 1$). It is also customary to set $\rho = 1$ in many (incompressible) simulations. Therefore, $4\pi\rho = 1$ in many simulations. If this is the case, we can use V_A and B_0 interchangeably for the Alfvén speed. Note that, in the units, kinetic energy density ($\rho v^2/2$) and magnetic energy density ($B^2/8\pi$) become $v^2/2$ and $B^2/2$, respectively. Hereinafter, we will call the system of units in which $4\pi\rho = 1$ ‘numerical’ units.

This regime of turbulence is called ‘strong’ MHD turbulence. On the other hand, if the strength of mean magnetic field is very strong, wave packets move very fast and thus duration of interaction will be very short. In this case, there will not be enough time to complete cascade. This type of turbulence is called ‘weak’ MHD turbulence. In this paper, we focus on strong MHD turbulence.

Energy spectrum and anisotropy are of great importance in MHD turbulence. Here, anisotropy means elongation of turbulence eddies (or wave packets). In incompressible hydrodynamic turbulence, the famous Kolmogorov theory (Kolmogorov 1941, 1962) assumes isotropy of eddy shapes and predicts

$$E_v(k) \propto k^{-5/3}, \quad (2)$$

where $E_v(k)$ is the kinetic energy spectrum. In incompressible MHD turbulence, Iroshnikov (1964) and Kraichnan (1965) assumed isotropy and derived $k^{-3/2}$ spectra for both velocity and magnetic field. However, the assumption of isotropy has received a lot of criticism (Montgomery and Turner 1981; Shebalin et al. 1983; Sridhar and Goldreich 1994; Montgomery and Matthaeus 1995; Matthaeus et al. 1998). In fact, it is natural for a dynamically important (i.e., strong) mean magnetic field to break a symmetry and provide a direction for anisotropy. Finally, Goldreich and Sridhar (1995, hereinafter GS95) proposed a theory on strong incompressible MHD turbulence, which predicts Kolmogorov spectra

$$E(k) \propto k^{-5/3}, \quad (3)$$

for both velocity and magnetic field, and scale-dependent anisotropy

$$l_{\parallel} \propto l_{\perp}^{2/3}, \quad (4)$$

where l_{\parallel} and l_{\perp} denote parallel and perpendicular sizes of an eddy, respectively. Later, numerical simulations confirmed the GS95 scaling relations (Cho and Vishniac 2000a; Maron and Goldreich 2001; Cho et al. 2002).

In this paper we review strong Alfvénic MHD turbulence in various environments. We consider not only the usual Alfvén wave but also its variants on small scales (i.e., whistler wave) and in the extreme relativistic limit (i.e., relativistic Alfvén wave). Except in Section 7, we assume incompressible fluids. In Section 2, we will briefly describe Kolmogorov theory for incompressible hydrodynamic turbulence. In Section 3, we consider strong incompressible Alfvénic MHD turbulence. In Section 4, we review weak incompressible MHD turbulence and show that, even in the case that large-scale turbulence is weak, strong MHD turbulence will ultimately emerge on a small scale. In Section 5, we adopt the electron MHD (EMHD) model and describe strong magnetized turbulence on a scale below the proton gyro-scale, where whistler waves, i.e., variants of Alfvén waves in the EMHD regime, interact and generate turbulence. In Sections 6 and 7, we briefly discuss strong relativistic Alfvénic turbulence and compressible MHD turbulence, respectively. In Section 8, we give conclusion.

2 Hydrodynamic turbulence

It may be useful to briefly review physical processes in incompressible hydrodynamic turbulence before we proceed to MHD turbulence. Detailed discussions on hydrodynamic turbulence can be found in [Frisch \(1995\)](#).

Turbulence is present in many astrophysical fluids. Why would we expect astrophysical fluids to be in turbulent state? A fluid with viscosity ν becomes turbulent when the rate of viscous dissipation, which is $\sim \nu/L^2$ at the energy injection scale L , is much smaller than the energy transfer rate $\sim v_L/L$, where v_L is the velocity dispersion at the scale L . The ratio of the two rates is the Reynolds number $Re = v_L L/\nu$. In general, astrophysical fluids have Re 's much larger than critical values, which is usually in the range from 10 to 100. Therefore, we expect turbulence in astrophysical fluids.

There exists a well-known empirical theory, i.e., Kolmogorov theory ([Kolmogorov 1941, 1962](#)), for incompressible hydrodynamic turbulence. In fully developed turbulence, eddies of various sizes interact each other. In Kolmogorov theory, kinetic energy contained in large-scale eddies cascades down to gradually smaller-scale eddies up to the viscosity scale (Figure 1). In this picture, it is important to know that the energy cascade rate is scale-independent. Let us assume that turbulence is in a statistically stationary state and focus on a scale l . If energy cascade rate from a larger scale to l is different from that from l to a smaller scale, energy on the scale l will either increase or decrease. In this case, we will not have a stationary state. Therefore, in order to have a stationary state, the energy cascade rate should be constant:

$$v_l^2/t_{cas} = \text{constant}, \quad (5)$$

where v_l is velocity fluctuation on the scale l and t_{cas} is energy cascade time on the scale. Note that v_l^2 is proportional to kinetic energy, since density is constant in incompressible medium.

It is possible to express t_{cas} in terms of l and v_l . A simple dimensional analysis gives

$$t_{cas} \sim l/v_l. \quad (6)$$

Physically speaking, l/v_l can be viewed as a quantity proportional to the rotation period of an eddy of size l and hence is called ‘eddy turnover time’. Note that v_l is velocity difference between two points separated by l . If we consider an eddy of size l , the velocity difference between two points that lie on the boundary of the eddy and separated by l is $\sim v_l$, which mean two points are moving away from each other at the speed of v_l (see Figure 1). In this picture, the eddy will be completely distorted after $t \sim l/v_l$. Therefore, l/v_l can also be viewed as distortion timescale of the eddy.

If we substitute Equation (6) into Equation (5), we have

$$v_l^3/l = \text{constant}, \quad (7)$$

or

$$v_l \propto l^{1/3}. \quad (8)$$

This relation is valid from energy injection scale (a.k.a. outer scale of turbulence) to viscosity scale (a.k.a. inner scale of turbulence).

If we perform Fourier transformation of velocity field $\mathbf{v}(\mathbf{r})$, we can obtain $\hat{\mathbf{v}}(\mathbf{k})$, where \mathbf{k} is the wavevector. Then the (volume-integrated) energy spectrum is

$$E_v(k) = \int |\hat{\mathbf{v}}(\mathbf{k})|^2 d^3\mathbf{k}, \quad (9)$$

where the integration is done over a spherical shell of unit thickness and radius k . If the energy spectrum follows a power law, then we have the relation

$$kE_v(k) \sim v_l^2. \quad (10)$$

Since $v_l^2 \propto l^{2/3} \propto k^{-2/3}$, we have

$$E_v(k) \propto k^{-5/3}, \quad (11)$$

which is called ‘Kolmogorov’ spectrum.

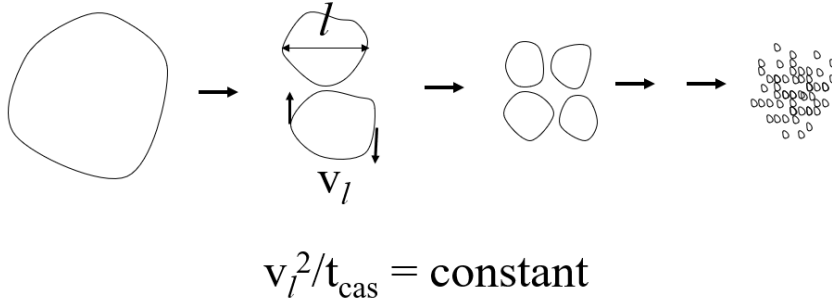


Fig. 1 Energy cascade in hydrodynamic turbulence.

3 Strong Alfvénic MHD turbulence

Let us consider MHD turbulence in a strongly magnetized incompressible medium. As we will see in Section 3.2, in the presence of a strong magnetic field, two physically meaningful timescales exist: nonlinear hydrodynamic timescale and wave-crossing timescale. In this section, we consider a special regime of turbulence called ‘strong’ MHD turbulence, in which two timescales have very similar values. If turbulence is driven isotropically, we need $v_L \sim V_A$ in order to have strong turbulence near the driving scale, where v_L is the velocity fluctuation on the driving scale L and V_A is the Alfvén speed. Note that $V_A = B_0$ in the system of units we adopt (i.e., numerical units) and $V_A = B_0 / \sqrt{4\pi\rho}$ in usual units. In the next section, we will show that ‘strong’ MHD turbulence will appear below a scale smaller than L even in the case of

$v_L < V_A$ in isotropically driven turbulence. Therefore, strong MHD turbulence may be regarded as a common type of MHD turbulence.

3.1 Interaction of Alfvén wave packets

It is well known that magnetic field lines have tension. Therefore, we may regard a magnetic field line as an elastic string. The restoring force for Alfvén wave is magnetic tension. If we properly perturb an elastic string, we can make the perturbation move along the string. Likewise, if we properly perturb magnetic field lines, we can generate an Alfvén wave packet that oscillates due to magnetic tension and we can make it move along the field lines. Note that we can make the Alfvén wave packet move either parallel or anti-parallel to the mean magnetic field.

The speed of Alfvén wave packet is B_0 in numerical units or $B_0/\sqrt{4\pi\rho}$ in usual units. Since all the Alfvén wave packets move at the same speed along the magnetic field, they do not interact. Therefore, Alfvén wave packets moving in one direction do not change their shapes in time, which means we can not have turbulence out of wave packets moving in one direction.

Mathematically, we can describe motion of Alfvén wave packets moving in one direction as follows. The MHD equations in incompressible medium are

$$\frac{\partial \mathbf{v}}{\partial t} = -\mathbf{v} \cdot \nabla \mathbf{v} + (B_0 \hat{\mathbf{z}} + \mathbf{b}) \cdot \nabla \mathbf{b} - \nabla P, \quad (12)$$

$$\frac{\partial \mathbf{b}}{\partial t} = -\mathbf{v} \cdot \nabla \mathbf{b} + \mathbf{b} \cdot \nabla \mathbf{v}, \quad (13)$$

where, \mathbf{v} is velocity, B_0 the strength of the mean magnetic field, $\hat{\mathbf{z}}$ the unit vector along z -direction, \mathbf{b} fluctuating magnetic field, and P the total pressure. We use numerical units for magnetic field, which means \mathbf{b} actually represents $\mathbf{b}/\sqrt{4\pi\rho}$. For simplicity, we ignore the viscosity and the magnetic dissipation terms. If we rewrite the equations in terms of Elsässer variables, $\mathbf{Z}^+ \equiv B_0 \hat{\mathbf{z}} + \mathbf{v} + \mathbf{b}$ and $\mathbf{Z}^- \equiv B_0 \hat{\mathbf{z}} + \mathbf{v} - \mathbf{b}$, we have

$$\frac{\partial \mathbf{Z}^+}{\partial t} - B_0 \frac{\partial \mathbf{Z}^+}{\partial z} = -\mathbf{Z}^- \cdot \nabla \mathbf{Z}^+ - \nabla P, \quad (14)$$

$$\frac{\partial \mathbf{Z}^-}{\partial t} + B_0 \frac{\partial \mathbf{Z}^-}{\partial z} = -\mathbf{Z}^+ \cdot \nabla \mathbf{Z}^- - \nabla P. \quad (15)$$

If \mathbf{Z}^- is zero, the nonlinear term in Equation (14) vanishes and we have

$$\frac{\partial \mathbf{Z}^+}{\partial t} - B_0 \frac{\partial \mathbf{Z}^+}{\partial z} = -\nabla P. \quad (16)$$

If we ignore the pressure gradient term², this becomes a wave equation for \mathbf{Z}^+ . The wave speed is constant (i.e., B_0), which means all waves have the same speed. If we

²The variable \mathbf{Z}^+ is incompressible, i.e., $\nabla \cdot \mathbf{Z}^+ = 0$, while the pressure gradient term is purely compressible. Therefore, generally speaking the pressure gradient term does not directly affect time evolution of \mathbf{Z}^+ in incompressible medium. It is also possible to show that ∇P is negligibly small in an Alfvénic perturbation with a small amplitude.

seek a solution of the form $\mathbf{Z}(k_z z + \omega t)$, we have $\omega = k_z B_0$, or

$$\omega = k_z V_A, \quad (17)$$

which means Alfvén waves are not dispersive and therefore Alfvén waves moving in one direction do not interact each other.

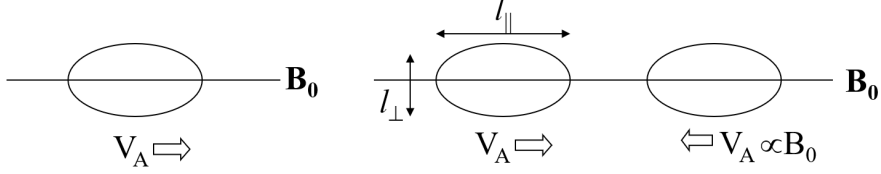


Fig. 2 Alfvén wave packets. (Left) An Alfvén wave packet moves at the Alfvén speed $V_A = B_0/\sqrt{4\pi\rho}$. When we use a system of units in which 4π does not appear and $\rho = 1$, it follows that $4\pi\rho = 1$ and hence $V_A = B_0$. Since Alfvén waves are non-dispersive, an Alfvén wave packet does not change its shape during the propagation in an incompressible fluid. (Right) When two opposite-traveling Alfvén wave packets collide, non-linear interactions happen.

Now, let us consider two opposite-traveling wave packets (see Figure 2). When they collide, they interact. Then, how can they interact? If we look at the time evolution of \mathbf{Z}^+ (see Equation (14)), the nonlinear interaction term $\mathbf{Z}^- \cdot \nabla \mathbf{Z}^+$ states that shearing motion provided by \mathbf{Z}^- distorts \mathbf{Z}^+ . Through the nonlinear process, smaller structures can be generated. If we drive turbulence on scale L , driving force generates opposite-traveling Alfvénic wave packets on scale L and collisions between them create smaller wave packets. Then, collisions between newly created smaller wave packets create even smaller wave packets. This ‘cascade’ process continues up to the dissipation scale and, this way, we have Alfvénic turbulence cascade.

3.2 Critical balance

In the previous subsection, we showed that collision of opposite-traveling wave packets (or ‘eddies’) is essential for Alfvénic turbulence. Based on the concept of critical balance, GS95 (Goldreich and Sridhar 1995) developed a theory on strong Alfvénic MHD turbulence. In this and next subsections, we briefly introduce critical balance and scaling relations by GS95.

Let us consider two opposite-traveling wave packets with similar sizes (see Figure 2). Let us assume that their sizes in the directions parallel and perpendicular to \mathbf{B}_0 are l_{\parallel} and l_{\perp} , respectively. We assume the cross-sectional shapes of the eddies are almost circular (i.e., isotropic) before the collision (see the left panel of Figure 3). During the collision, an eddy is distorted by shearing motion of the other eddy. Here, we only consider distortion in the perpendicular direction. If velocity difference between two points, whose perpendicular separation is l_{\perp} , is v_l , then the distortion timescale is

$$t_{eddy} \sim l_{\perp}/v_l, \quad (18)$$

which is none other than the eddy turnover time of hydrodynamic turbulence. Note that, when an eddy is completely distorted, it will become different scale (i.e., smaller scale) eddies through nonlinear interactions, which means energy cascade is completed from scale l_{\perp} to a smaller scale. On the other hand, the duration of collision is equal to the parallel size divided by the wave speed:

$$t_{wave} \sim l_{\parallel}/V_A. \quad (19)$$

If $t_{eddy} \sim t_{wave}$, an eddy becomes completely distorted after one collision, which means that one collision is enough to complete energy cascade. The condition $t_{eddy} \sim t_{wave}$ is called ‘critical balance’ and ‘critically balanced’ turbulence is called ‘strong’ MHD turbulence. From Equations (18) and (19), the condition for strong MHD turbulence becomes

$$\frac{l_{\perp}}{v_l} \sim \frac{l_{\parallel}}{V_A}. \quad (20)$$

If turbulence driving is isotropic, we expect $L_{\parallel} \sim L_{\perp}$ at the driving scale L . In this case, the condition for strong MHD turbulence at the driving scale is

$$V_A \sim v_L, \quad (21)$$

which means that the Alfvén Mach number is unity:

$$M_A \equiv \frac{v_L}{V_A} \sim 1. \quad (22)$$

The condition for critical balance in Equation (20) or (21) looks very special and hard to fulfill. However, in next section, we will show that even in the case of $t_{eddy} > t_{wave}$ on the driving scale, we will ultimately have the condition met on smaller scales.

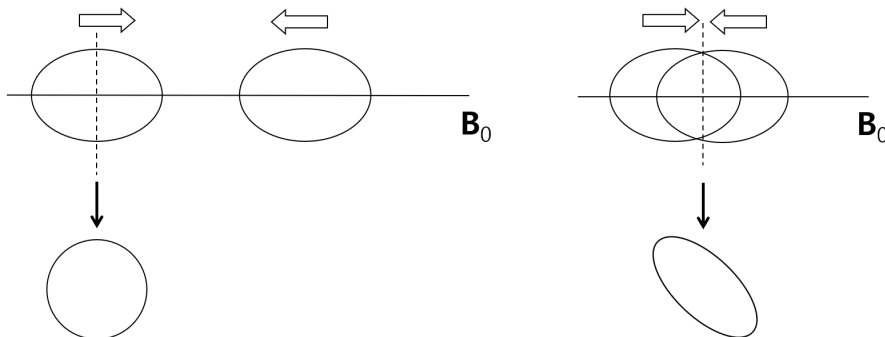


Fig. 3 Collision of wave packets. Shapes shown below the arrows are cross-sectional shapes. (Left) Before the collision, we assume perpendicular shapes of the eddies are isotropic. (Right) During the collision, an eddy is distorted by shearing motion of the other eddy.

3.3 Scaling relations in strong Alfvénic turbulence

As in hydrodynamic turbulence, we can assume constancy of energy cascade rate. By combining constancy of energy cascade rate and critical balance, we can derive energy spectrum and anisotropy of strong Alfvénic turbulence:

- Constancy of energy cascade rate:

$$v_l^2/t_{cas} = \text{constant}, \quad (23)$$

- Critical balance:

$$\frac{l_\perp}{v_l} \sim \frac{l_\parallel}{V_A}. \quad (24)$$

In Equation (23), v_l^2 is proportional to kinetic energy density on scale l . Since $v_l \sim b_l$ in Alfvén wave packets, either v_l^2 or b_l^2 can be used in the equation.

There are two physically meaningful timescales in MHD: hydrodynamic timescale ($t_{eddy} \sim l_\perp/v_l$) and wave-crossing timescale ($t_{wave} \sim l_\parallel/V_A$). Since two timescales are virtually same (see Equation (24)) in strong turbulence, we can use either of them for t_{cas} . If we use l_\perp/v_l for t_{cas} , Equation (23) becomes

$$v_l^3/l_\perp = \text{constant}. \quad (25)$$

As in hydrodynamic turbulence, the kinetic energy spectrum corresponding to Equation (25) is

$$E_v(k) \propto k^{-5/3}. \quad (26)$$

Since $v_l \sim b_l$ in Alfvén wave packets, we also have a Kolmogorov spectrum for magnetic field:

$$E_b(k) \sim E_v(k) \propto k^{-5/3}. \quad (27)$$

If we substitute Equation (25) into Equation (24), we have

$$l_\parallel \propto l_\perp^{2/3}. \quad (28)$$

Note that l_\parallel and l_\perp denote parallel and perpendicular sizes of an eddy, respectively. Therefore, Equation (28) tells us anisotropy of eddy shape: smaller eddies are more elongated along the (local) mean field direction.

In summary, we use constancy of energy cascade rate and critical balance to derive scaling relations of strong Alfvénic turbulence. The result shows that strong Alfvénic turbulence has Kolmogorov spectra for both velocity and magnetic field and scale-dependent anisotropy of eddy shape.

3.4 Numerical tests and observations

Using numerical simulations, [Cho and Vishniac \(2000a\)](#) first tested the theory of strong MHD turbulence. We numerically solved the incompressible MHD equations in

a periodic box and calculated spectrum and anisotropy. We used isotropic large-scale driving to generate strong MHD turbulence.

Figure 4 shows results from a simulation in [Cho and Vishniac \(2000a\)](#). The left panel of Figure 4 visualizes three-dimensional distribution of $|\mathbf{B}|$. The right panel of the figure shows kinetic and magnetic spectra. Although the magnetic spectrum (dotted line) is slightly shallower than the kinetic one (solid line), the overall spectra are roughly consistent with Kolmogorov spectrum.

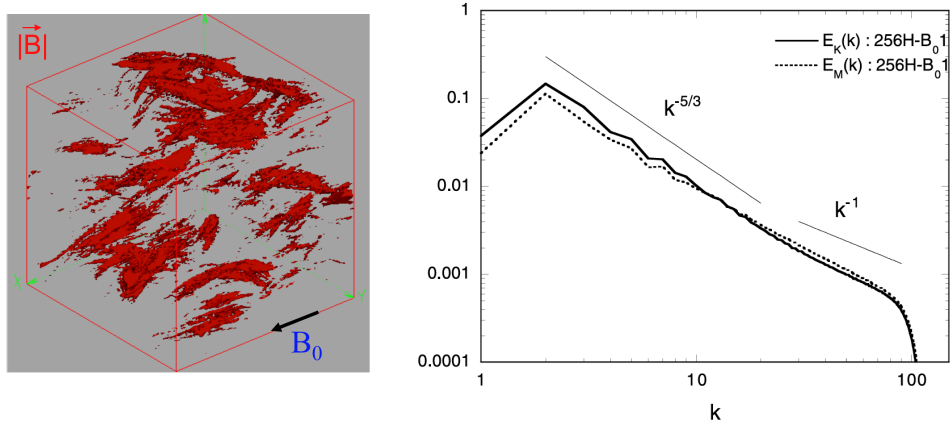


Fig. 4 (Left) Snapshot of magnetic field strength. The black arrow represents the direction of the mean magnetic field. (Right) Kinetic and magnetic spectra. They are compatible with Kolmogorov spectrum and hence agree with the GS95 prediction. From [Cho and Vishniac \(2000a\)](#).

Figure 5 shows anisotropy of strong MHD turbulence. The left panel of Figure 5 demonstrates scale-dependent anisotropy. Large-scale eddies (see, for example, the white ellipse) are more or less isotropic. However, small-scale eddies (see, for example, the green ellipse) are highly elongated. [Cho and Vishniac \(2000a\)](#) devised a method to quantitatively measure the parallel and perpendicular sizes of eddies. According to GS95, the parallel and perpendicular sizes of eddies follow the relation $l_{\parallel} \propto l_{\perp}^{2/3}$. The right panel of Figure 5 shows that the relation holds true. The horizontal and vertical axes correspond to l_{\perp} and l_{\parallel} , respectively.

Measurements of solar wind magnetic spectrum have a long history (for review, see, e.g., [Bruno and Carbone 2013](#)). Although there are some uncertainties, the results are mostly compatible with the GS95 prediction. Scale-dependent anisotropy has been measured only recently and the results are consistent with the GS95 anisotropy (see, for example, [Horbury et al. 2008](#); [Podesta 2009](#); [Wicks et al. 2010](#); see also a review by [Chen 2016](#)).

3.5 Further developments in strong Alfvénic turbulence research

In this section, we only focus on simple and basic physics of strong MHD turbulence. However, there are many complicated aspects of strong MHD turbulence. For example,

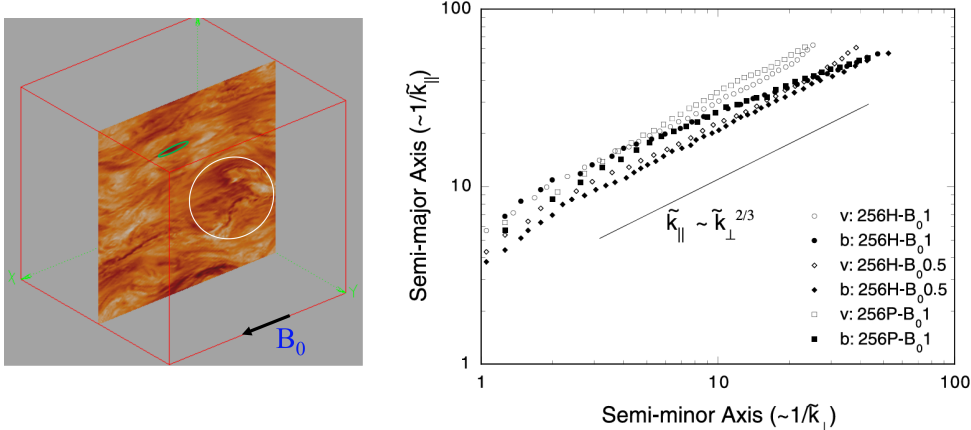


Fig. 5 (Left) Illustration of scale-dependent anisotropy. The black arrow represents the direction of the mean magnetic field. (Right) Measured anisotropy of eddy shapes. The parallel and perpendicular sizes of eddies, l_{\parallel} and l_{\perp} respectively, follow the relation $l_{\parallel} \propto l_{\perp}^{2/3}$, which agrees with the GS95 prediction. From [Cho and Vishniac \(2000a\)](#).

when we considered collision of opposite-traveling wave packets, we tacitly assumed that they have similar amplitudes (i.e., similar values for $|\mathbf{b}_i|$). However, in reality, they can have different amplitudes. This kind of turbulence is called ‘imbalanced’ turbulence ([Lithwick et al. 2007](#); [Beresnyak and Lazarian 2008, 2009](#); [Chandran 2008a](#); [Perez and Boldyrev 2009](#); [Podesta and Bhattacharjee 2010](#); [Perez et al. 2012](#); [Mason et al. 2012](#); [Cho and Lazarian 2014a](#)). There are also claims that alignment between variables (e.g., Elsässer variables \mathbf{Z}^+ and \mathbf{Z}^-) can modify energy spectrum of strong MHD turbulence ([Boldyrev 2005, 2006](#); [Beresnyak and Lazarian 2006](#); [Beattie and Bhattacharjee 2025](#)). There are also other issues related to strong MHD turbulence (see reviews by [Beresnyak \(2019\)](#) and [Schekochihin \(2022\)](#) for further details).

4 MHD turbulence with a very strong mean magnetic field

In the previous section, we introduced strong Alfvénic MHD turbulence, which is based on critical balance. In case of isotropic driving, the condition for critical balance is $V_A \sim v_L$. However, if the mean magnetic field is very strong, it is possible to have $V_A > v_L$ for isotropic driving, or $V_A L_{\perp} / v_L L_{\parallel} > 1$ for general cases. This type of turbulence is called ‘weak’ MHD turbulence. In case of isotropic driving, the Alfvén Mach number ($M_A \equiv v_{rms} / V_A$) is less than unity in weak turbulence. Therefore, weak MHD turbulence virtually coincides with sub-Alfvénic turbulence if driving is isotropic. In this section, we will show that critical balance is satisfied below the scale $\sim LM_A^2$, even if $V_A \gg v_L$.

[Zakharov et al. \(1992\)](#) provided general discussions on weak turbulence. [Goldreich and Sridhar \(1997\)](#) and [Ng and Bhattacharjee \(1997\)](#) derived the spectrum of weak

turbulence using scaling arguments. Galtier (2000) first developed kinetic theory for weak turbulence.

4.1 Cascade time in weak turbulence

In weak turbulence, $t_{eddy} > t_{wave}$. Since the time necessary for complete distortion (i.e., t_{eddy}) is longer than duration of collision (i.e., t_{wave}), an eddy cannot be completely distorted after one collision, which means that more than one collisions are necessary for complete distortion of the eddy. Therefore, more than one collision is necessary to complete energy cascade.

Then how many collisions are necessary? The magnetic induction equation reads

$$\frac{\partial \mathbf{B}}{\partial t} = \nabla \times (\mathbf{v} \times \mathbf{B}) + \eta \nabla^2 \mathbf{B}, \quad (29)$$

where $\mathbf{B} = \mathbf{B}_0 + \mathbf{b}$ and η is magnetic diffusivity. From this, we can write

$$\frac{db_l}{dt} \sim \frac{b_l v_l}{l_\perp}, \quad (30)$$

where we assume derivative in the direction perpendicular to the (local) mean magnetic field is larger than the one in the parallel direction due to anisotropy of turbulence in the presence of strong mean magnetic field. Here we also assume locality of nonlinear interactions: i.e., time evolution of an eddy of size l is determined by interactions with similar-size eddies and thus the magnitude of the nonlinear term on scale l is $|\nabla \times (\mathbf{v} \times \mathbf{b})| \sim v_l b_l / l_\perp$. Since $v_l \sim b_l$, we can rewrite (30) as follows:

$$\frac{dv_l}{dt} \sim \frac{v_l^2}{l_\perp}. \quad (31)$$

From Equation (31), we have

$$\frac{d\mathcal{E}_l}{dt} \sim \frac{v_l^3}{l_\perp}, \quad (32)$$

where $\mathcal{E}_l \sim v_l^2$ is energy density on scale l . The change in energy during one collision is

$$|\Delta \mathcal{E}_l| \sim (d\mathcal{E}_l/dt)\Delta t \sim (v_l^3/l_\perp)t_{wave} \sim (v_l^3/l_\perp)(l_\parallel/V_A), \quad (33)$$

and, therefore, we have

$$\frac{|\Delta \mathcal{E}_l|}{\mathcal{E}_l} \sim \frac{v_l l_\parallel}{V_A l_\perp} = \frac{t_{wave}}{t_{eddy}} \equiv \chi < 1. \quad (34)$$

Equation (34) confirms that many collisions are necessary to complete energy cascade in weak Alfvénic turbulence. If each collision contributes to energy change randomly, then the number of collisions required for energy cascade will be

$$N \sim (1/\chi)^2. \quad (35)$$

Therefore, the cascade time becomes

$$t_{cas} \sim N t_{wave} \sim (t_{eddy}/t_{wave})^2 t_{wave} = (t_{eddy}/t_{wave}) t_{eddy} = (V_A l_{\perp}^2 / v_t^2 l_{\parallel}). \quad (36)$$

4.2 Anisotropy of weak MHD turbulence

Since $t_{eddy} > t_{wave}$, wave-like motions and wave-wave interactions are important in weak turbulence. Many researchers have argued that wave-wave interactions result in strong anisotropy (see, for example, Shebalin et al. 1983; Sridhar and Goldreich 1994; Montgomery and Matthaeus 1995). Mathematically, anisotropy manifests itself in the resonant conditions for 3-wave interactions:

$$\mathbf{k}_1 + \mathbf{k}_2 = \mathbf{k}_3, \quad (37)$$

$$\omega_1 + \omega_2 = \omega_3, \quad (38)$$

where \mathbf{k} 's are wavevectors and ω 's are wave frequencies. If we rewrite Equation (37) only for the parallel direction and Equation (38) using $\omega = V_A |k_{\parallel}|$ (see Alfvén-wave dispersion relation in Equation (17)), we have

$$k_{\parallel,1} + k_{\parallel,2} = k_{\parallel,3}, \quad (39)$$

$$|k_{\parallel,1}| + |k_{\parallel,2}| = |k_{\parallel,3}|, \quad (40)$$

where k_{\parallel} 's are parallel wavenumbers.

Since only opposite-traveling wave packets interact, $k_{\parallel,1}$ and $k_{\parallel,2}$ must have opposite signs. Suppose that $k_{\parallel,3}$ is positive. In this case, there two solutions for Equations (39) and (40): either $k_{\parallel,1} = 0$ and $k_{\parallel,2} = k_{\parallel,3}$ or $k_{\parallel,2} = 0$ and $k_{\parallel,1} = k_{\parallel,3}$. In the case of $k_{\parallel,1} = 0$ and $k_{\parallel,2} = k_{\parallel,3}$, energy in wave 2 is transferred to wave 3 by the help of wave 1. Since k_{\parallel} of 'donor' is the same as that of 'recipient', the parallel wavenumber (k_{\parallel}) does not change during the cascade:

$$k_{\parallel} = \text{constant}, \quad (41)$$

which means that the parallel size of an eddy does not change during the cascade. Only the perpendicular size reduces during the cascade.

4.3 Scaling relation of weak MHD turbulence

By combining constancy of energy cascade rate, the expression for t_{cas} in Equation (36), and anisotropy in Equation (41), we can derive energy spectrum and anisotropy of weak Alfvénic turbulence:

- Constancy of energy cascade rate:

$$v_t^2 / t_{cas} = \text{constant}, \quad (42)$$

- Expression for t_{cas} :

$$t_{cas} \sim \left(\frac{t_{eddy}}{t_{wave}} \right) t_{eddy} = \frac{V_A l_{\perp}^2}{v_l^2 l_{\parallel}}. \quad (43)$$

- Anisotropy:

$$k_{\parallel} = \text{constant}. \quad (44)$$

If we insert Equation (43) into Equation (42), we have

$$v_l^2 (v_l^2 l_{\parallel} / V_A l_{\perp}^2) = \text{constant}, \text{ or } v_l^2 \propto l_{\perp}, \quad (45)$$

where we use the fact that k_{\parallel} is constant (Equation (44)). Since $kE_v(k) \sim v_l^2$ (see Equation (10)), we have the following energy spectrum:

$$E_v(k) \propto k_{\perp}^{-2}. \quad (46)$$

Since $v_l \sim b_l$ for Alfvénic perturbations, we also have a k_{\perp}^{-2} spectrum for magnetic field.

4.4 Transition from weak to strong turbulence on a small scale

In weak turbulence, $\chi < 1$ on the driving scale. From Equation (45), we have

$$v_l = v_L (l_{\perp} / L)^{1/2}, \quad (47)$$

where $v_L \sim v_{rms}$ is the velocity on the driving scale L . Using this, we can write χ on scale l_{\perp} :

$$\chi = \frac{v_l l_{\parallel}}{V_A l_{\perp}} = \frac{v_L L_{\parallel}}{V_A l_{\perp}^{1/2} L^{1/2}} \sim \frac{v_L}{V_A} \left(\frac{L}{l_{\perp}} \right)^{1/2}, \quad (48)$$

where we use $l_{\parallel} = L_{\parallel} \sim L$. This equation tells us that χ increases as l_{\perp} decreases and χ becomes unity on the scale

$$l_{\perp} \sim (v_L / V_A)^2 L = M_A^2 L. \quad (49)$$

Therefore, transition from weak to strong turbulence happens on this scale. Below the transition scale, critical balance is satisfied and we can use the scaling relations for strong MHD turbulence. In Figure 6, we illustrate this transition in Fourier space. Transition from weak to strong turbulence is observed in direct numerical simulations (Meyrand et al. 2016) and also in space plasmas (Zhao et al. 2024).

5 Small-scale MHD Turbulence

We can use MHD to describe large-scale motions. However, on sufficiently small scales, MHD approximation will ultimately fail and we cannot apply the theory of MHD turbulence to the small scales. In the solar wind, for example, the slope of magnetic

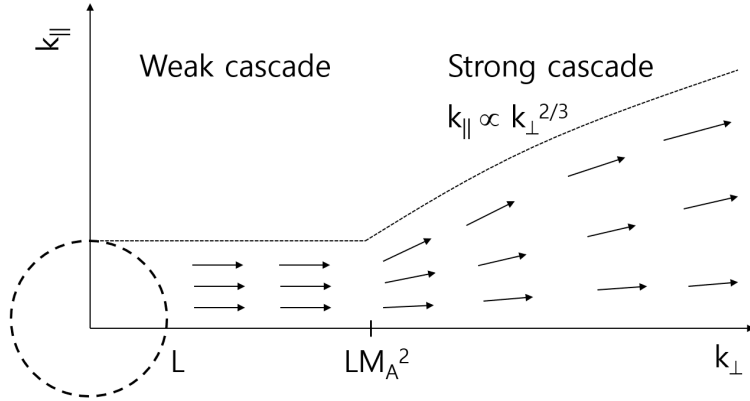


Fig. 6 Transition from weak to strong cascade on the scale $\sim LM_A^2$, where $M_A = v_L/B_0$ is the Alfvén Mach number.

energy spectrum changes near the proton gyro-scale. The magnetic energy spectrum is consistent with Kolmogorov one above the gyro-scale, while it is much steeper than Kolmogorov one below the gyro-scale (see illustration in the left panel of Figure 9). The scales below the MHD scale are sometimes called ‘dispersion range’ since waves in the range are dispersive. The power index of the energy spectrum in the dispersion range usually varies between -2 and -4 (see, for example, Leamon et al. 1998; Leamon et al. 1999; Smith et al. 2006). Understanding physics of the dispersion range is of great importance in space physics (Dmitruk and Matthaeus 2006; Howes et al. 2008; Matthaeus et al. 2008; Howes et al. 2008; Saito et al. 2008; Schekochihin et al. 2009).

In this section, we use Electron MHD (EMHD) to understand physics of small-scale turbulence. EMHD is a very simple fluid-like model to describe small-scale physics (Kingsep et al. 1990). As early as 1990s, researchers found a steep energy spectrum ($E(k) \propto k^{-7/3}$) for EMHD turbulence (Biskamp et al. 1996, 1999; Ng et al. 2003). There are also studies on anisotropic nature of (two-dimensional) EMHD turbulence (Dastgeer and Zank 2003; Ng et al. 2003). In 2004, Cho and Lazarian first derived scale-dependent anisotropy of three-dimensional strong EMHD turbulence based on critical balance. In this section, we only consider strong EMHD turbulence. Discussions on weak EMHD turbulence can be found in Galtier and Bhattacharjee (2003), Galtier and Bhattacharjee (2005) and Galtier (2006).

5.1 Electron MHD model

EMHD assumes that protons provide smooth charge background and only electrons carry current on scales below the proton gyro-scale (see the right panel of Figure 7). Therefore, since electron motions generate current, current density is proportional to electron velocity:

$$\mathbf{J} = -nev, \quad (50)$$

where n is electron number density, e is electric charge, and \mathbf{v} is electron velocity. Note that electron velocity here does not mean velocity of individual electron, but

bulk velocity of electron ‘fluid’. From Equation (50), we have

$$\mathbf{v} = -\frac{\mathbf{J}}{ne} = -\frac{c}{4\pi ne}\nabla \times \mathbf{B}. \quad (51)$$

To derive the EMHD equation, let us start with magnetic induction equation

$$\frac{\partial \mathbf{B}}{\partial t} = \nabla \times (\mathbf{v} \times \mathbf{B}) + \eta \nabla^2 \mathbf{B}. \quad (52)$$

If we substitute Equation (51) into Equation (52), we have

$$\frac{\partial \mathbf{B}}{\partial t} = -\frac{c}{4\pi ne}\nabla \times [(\nabla \times \mathbf{B}) \times \mathbf{B}] + \eta \nabla^2 \mathbf{B}. \quad (53)$$

Although we do not go into details, we can simplify Equation (53) by properly normalizing magnetic field, time, and length (see, for example, [Galtier and Bhattacharjee 2003](#)):

$$\frac{\partial \mathbf{B}}{\partial t} = -\nabla \times [(\nabla \times \mathbf{B}) \times \mathbf{B}] + \eta' \nabla^2 \mathbf{B}. \quad (54)$$

This is the equation for EMHD ([Kingsep et al. 1990](#)). In EMHD, velocity is not an independent variable and, therefore, we do not need an equation for velocity. We can derive velocity from magnetic field using Equation (51).

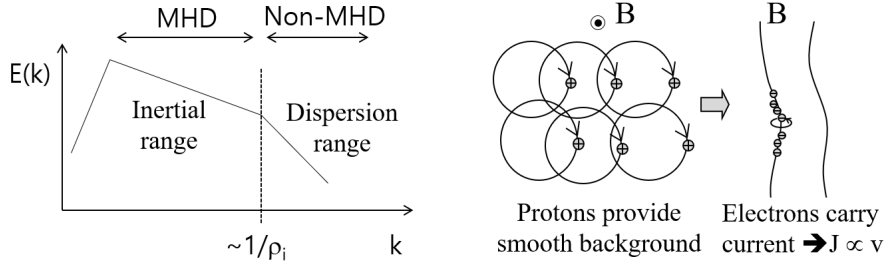


Fig. 7 (Left) Change of energy spectrum near the proton gyro-scale ρ_i . (Right) Electron MHD model. Protons provide smooth charge background and only electrons carry current.

5.2 Speed of EMHD waves

Let us assume

$$\mathbf{B} = \mathbf{B}_0 + \mathbf{b}, \quad (55)$$

where we assume \mathbf{B}_0 is a constant vector and $B_0 \equiv |\mathbf{B}_0| \gg |\mathbf{b}|$. If we substitute this into the EMHD equation (Equation (54)), we have

$$\frac{\partial \mathbf{b}}{\partial t} = -\nabla \times [(\nabla \times \mathbf{b}) \times \mathbf{B}_0], \quad (56)$$

where we ignore the second-order term and the magnetic diffusion term. The term on the right-hand side has the form $\nabla \times (\mathbf{j} \times \mathbf{B}_0)$ with $\mathbf{j} = \nabla \times \mathbf{b}$. Since $\nabla \cdot \mathbf{j} = 0$ and \mathbf{B}_0 is a constant vector, the vector identity

$$\nabla \times (\mathbf{j} \times \mathbf{B}_0) = \mathbf{j}(\nabla \cdot \mathbf{B}_0) - \mathbf{B}_0(\nabla \cdot \mathbf{j}) + (\mathbf{B}_0 \cdot \nabla)\mathbf{j} - (\mathbf{j} \cdot \nabla)\mathbf{B}_0 \quad (57)$$

becomes

$$\nabla \times (\mathbf{j} \times \mathbf{B}_0) = (\mathbf{B}_0 \cdot \nabla)\mathbf{j} = (\mathbf{B}_0 \cdot \nabla)(\nabla \times \mathbf{b}) \quad (58)$$

and Equation (56) becomes

$$\frac{\partial \mathbf{b}}{\partial t} = -(\mathbf{B}_0 \cdot \nabla)(\nabla \times \mathbf{b}). \quad (59)$$

EMHD waves are actually whistler waves. A whistler is circularly polarized. In Fourier space, the bases that describe circular polarization are

$$\hat{\epsilon}_+ \equiv (\hat{\mathbf{s}}_1 + i\hat{\mathbf{s}}_2)/\sqrt{2} \text{ and } \hat{\epsilon}_- \equiv (\hat{\mathbf{s}}_1 - i\hat{\mathbf{s}}_2)/\sqrt{2}, \quad (60)$$

where $\hat{\mathbf{s}}_1$ and $\hat{\mathbf{s}}_2$ are orthogonal unit vectors perpendicular to \mathbf{k} and we assume $\hat{\mathbf{s}}_1 \times \hat{\mathbf{s}}_2 = \hat{\mathbf{k}} \equiv \mathbf{k}/k$. The $+$ waves move in the positive direction and the $-$ waves in the negative (i.e., opposite) direction with respect to \mathbf{B}_0 . Let us consider a $+$ wave: $\tilde{\mathbf{b}}_{\mathbf{k}} = b_0 \exp(-i\omega t)\hat{\epsilon}_+$, where b_0 is a constant. In Fourier space, $\nabla \rightarrow i\mathbf{k}$ and Equation (59) becomes

$$-i\omega\hat{\epsilon}_+ = -B_0 i k_{\parallel} i\mathbf{k} \times (\hat{\mathbf{s}}_1 + i\hat{\mathbf{s}}_2)/\sqrt{2} = -iB_0 k k_{\parallel} \hat{\epsilon}_+, \quad (61)$$

where $B_0 k_{\parallel} = \mathbf{B}_0 \cdot \mathbf{k}$ and we use $\hat{\mathbf{k}} \times \hat{\mathbf{s}}_1 = \hat{\mathbf{s}}_2$ and $\hat{\mathbf{k}} \times \hat{\mathbf{s}}_2 = -\hat{\mathbf{s}}_1$. Therefore we have the dispersion relation

$$\omega = k k_{\parallel} B_0 = k^2 B_0 \cos \theta, \quad (62)$$

where θ is the angle between \mathbf{B}_0 and \mathbf{k} . Alfvén waves, which have the dispersion relation $\omega = k_{\parallel} V_A = k V_A \cos \theta$, propagate along the magnetic field at the Alfvén speed V_A ($= B_0$ in numerical units). Therefore, we can conclude that a whistler wave (with a wavenumber k) propagates along the magnetic field at the speed of $k V_A$ ($= k B_0$ in numerical units). Since the propagation speed depends on the wavenumber k , whistler waves are dispersive.

5.3 Critical balance in strong EMHD turbulence

As we have seen in the previous subsection, whistler waves (i.e., EMHD waves) are dispersive. Therefore, whistler wave packets moving in one direction can interact each other and generate turbulence. However, this process is relatively slow and results in inverse cascade (see [Schekochihin et al. 2009](#); [Cho 2011](#); [Kim and Cho 2015](#)) rather than usual forward cascade. Therefore, as in Alfvénic MHD turbulence, let us only consider opposite-traveling wave packets with similar sizes (see [Figure 8](#)). Let us assume that their sizes in the directions parallel and perpendicular to \mathbf{B}_0 are l_{\parallel} and l_{\perp} , respectively. To derive scaling relations in EMHD turbulence, we can simply follow

the arguments in Sections 3.2 and 3.3. We can use Figure 3 not only for MHD but also for EMHD. Note, however, that there are two important differences between MHD and EMHD. First, the wave propagation speed is B_0 in MHD and kB_0 in EMHD. Second, $v_l \sim b_l$ in MHD and $v_l = \nabla \times \mathbf{b} \sim b_l/l_\perp$ in EMHD. Here we assume that turbulence structures are elongated along the direction parallel to magnetic field and, hence, derivative in perpendicular direction is larger than that in parallel direction.

We assume the cross-sectional shapes of the EMHD eddies are almost circular (i.e., isotropic) before the collision (see the left panel of Figure 3). During the collision, an EMHD eddy is distorted by shearing motion of the other EMHD eddy. Here, we only consider distortion in the perpendicular direction. If velocity difference between two points, whose perpendicular separation is l_\perp , is v_l , then the distortion timescale is

$$t_{eddy} \sim l_\perp/v_l \sim l_\perp^2/b_l. \quad (63)$$

On the other hand, the duration of collision is equal to the parallel size divided by the wave speed:

$$t_{wave} \sim l_\parallel/(kV_A) = l_\parallel l_\perp/B_0, \quad (64)$$

where we assume $k = (k_\perp^2 + k_\parallel^2)^{1/2} \sim k_\perp \sim 1/l_\perp$.

As in MHD, let us assume critical balance: $t_{eddy} \sim t_{wave}$. Note that, if $t_{eddy} \sim t_{wave}$, an eddy becomes completely distorted after one collision and, therefore, one collision is enough for energy cascade. From Equations (63) and (64), the condition for critical balance, hence for strong EMHD turbulence, becomes

$$\frac{l_\perp}{b_l} \approx \frac{l_\parallel}{B_0}, \quad (65)$$

which is identical to the one for MHD, if the latter is expressed in terms of b_l rather than v_l . If turbulence driving is isotropic, the condition for critical balance at the driving scale is

$$B_0 \sim b_L \sim b_{rms}. \quad (66)$$

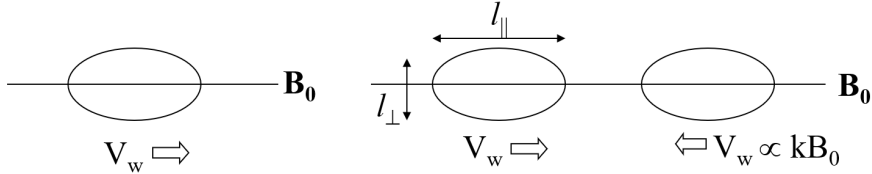


Fig. 8 (Left) An EMHD wave packet (i.e., a whistler wave packet) moving in one direction. (Right) Two opposite-traveling EMHD wave packets. The propagation speed of an EMHD wave (i.e., whistler wave) is kV_A , which is equal to kB_0 in the numerical units we adopt.

5.4 Scaling relations in strong EMHD turbulence

By combining constancy of energy cascade rate and critical balance, we can derive energy spectrum and anisotropy of strong EMHD turbulence:

- Constancy of energy cascade rate:

$$b_l^2/t_{cas} = \text{constant}, \quad (67)$$

- Critical balance (i.e., $t_{eddy} = t_{wave}$):

$$\frac{l_\perp^2}{b_l} \sim \frac{l_\parallel l_\perp}{B_0}. \quad (68)$$

Since two physically meaningful timescales, i.e., t_{eddy} and t_{wave} , are similar (see Equation (68)), we can use either of them for t_{cas} . If we use l_\perp^2/b_l for t_{cas} , Equation (67) becomes

$$b_l^3/l_\perp^2 = \text{constant}, \text{ or } b_l^2 \propto l_\perp^{4/3}. \quad (69)$$

The magnetic energy spectrum corresponding to Equation (69) is

$$E_b(k) \propto k^{-7/3}. \quad (70)$$

If we substitute Equation (69) into Equation (68), we have

$$l_\parallel \propto l_\perp^{1/3}. \quad (71)$$

Note that anisotropy in strong MHD turbulence is $l_\parallel \propto l_\perp^{2/3}$. Therefore, Equation (71) states that anisotropy in EMHD turbulence is stronger than that in MHD one.

In summary, we use constancy of energy cascade rate and critical balance to derive scaling relations in strong EMHD turbulence. The results shows that strong EMHD turbulence has a spectrum steeper than the Kolmogorov spectrum and anisotropy stronger than its MHD counterpart.

5.5 Numerical tests of strong EMHD turbulence theory

[Cho and Lazarian \(2004\)](#) first developed and numerically tested the theory of strong MHD turbulence. They performed a numerical simulation of decaying EMHD turbulence. At $t = 0$, the random magnetic field is restricted to the range $2 \leq k \leq 4$ in wavevector (\mathbf{k}) space and the amplitude of the random magnetic field is very close to that of the mean magnetic field (i.e., $b \sim B_0$). Therefore, the condition for critical balance is satisfied at $t = 0$.

The left panel of Figure 9 shows that the initial energy (see the dotted line) cascades down to small scales as time goes on. At $t = 0.33$, energy has already reached the dissipation scale (see the dashed line). After energy has reached the dissipation

scale, the energy spectrum decreases without changing the spectral slope (compare the dashed and the solid lines). Condition for strong turbulence is maintained for t 's shown in the left panel. The power index of energy spectrum is consistent with $-7/3$. The right panel of Figure 9 displays anisotropy, which also confirms the theoretical prediction $l_{\parallel} \propto l_{\perp}^{1/3}$. Higher resolutions runs in Cho and Lazarian (2009) also confirm these findings.

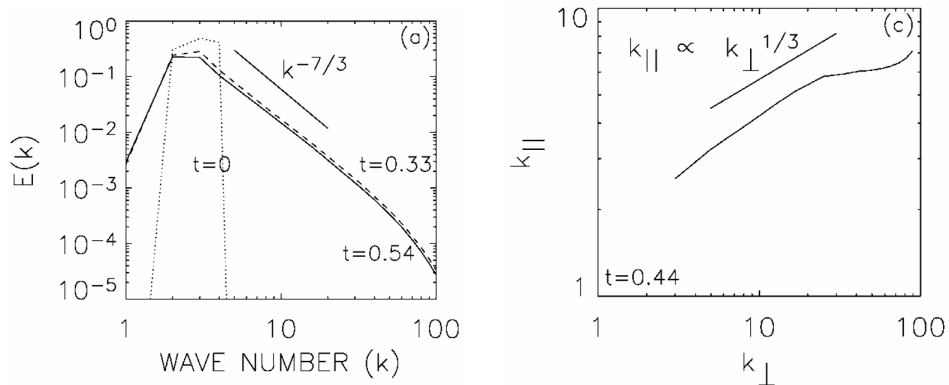


Fig. 9 (Left) Spectra of decaying EMHD turbulence. (Right) Anisotropy. From Cho and Lazarian (2004).

6 Relativistic Alfvénic MHD Turbulence

If magnetic field is sufficiently strong, it is possible that magnetic energy density is much larger than that of matter: $B^2/8\pi \gg \rho c^2$. This may be the case in magnetosphere of a pulsar or a black hole (see, for example, Goldreich and Julian 1969; Blandford and Znajek 1977; Duncan and Thompson 1992) or in gamma-ray bursts (see, for example, Thompson 1994; Lyutikov and Blandford 2003). If this is the case, the Alfvén speed approaches the speed of light, and we need relativity to describe physics of the system. If we completely ignore the energy density of matter, the Lorentz force vanishes and hence we can use the relativistic force-free approximation. As in the non-relativistic case, Alfvén waves in this extreme relativistic limit propagate at the same speed (in fact, at the speed of light) along the magnetic field line and hence those moving in the same direction do not interact. Thompson and Blaes (1998) proposed a theory on strong MHD turbulence in this regime. According to the theory, spectrum and anisotropy of the relativistic MHD turbulence is virtually identical to those of its non-relativistic counterpart: $E_b \propto k^{-5/3}$ and $k_{\parallel} \propto l_{\perp}^{2/3}$. Cho (2005) numerically confirmed the scaling relations. In this section, we briefly introduce relativistic force-free MHD turbulence.

6.1 Critical balance in relativistic Alfvénic turbulence

An Alfvén wave propagates at the speed of light (i.e., $V_A = c$) along the magnetic field in the relativistic force-free regime. Consider an Alfvén wave packet moving to the left (see Figure 10). Let its parallel and perpendicular sizes be l_{\parallel} and l_{\perp} , respectively. Since the strength of fluctuating magnetic field on scale the scale is $\sim b_l$, typical inclination of a magnetic field line on the scale with respect to the mean field is $\sim b_l/B_0$ (see the middle panel of Figure 10). When the wave packet moves to the left, a point on the magnetic field line will move up and down at the speed of

$$v_l \sim c(b_l/B_0). \quad (72)$$

Using the facts that $V_A = c$ and that $v_l \sim c(b_l/B_0)$, we can derive scaling relations for strong Alfvénic turbulence in the regime. As in the non-relativistic MHD, let us consider two opposite-traveling wave packets (see Figure 2). When they collide, they interact and generate a turbulence cascade. We assume the cross-sectional shapes of the relativistic Alfvén eddies are almost circular (i.e., isotropic) before the collision (see the left panel of Figure 3). During the collision, the eddy is distorted by shearing motion of the other eddy. Here, we only consider distortion in the perpendicular direction. Then, the distortion timescale is

$$t_{eddy} \sim l_{\perp}/v_l \sim l_{\perp}/(cb_l/B_0) = l_{\perp}B_0/cb_l. \quad (73)$$

On the other hand, the duration of collision is equal to the parallel size divided by the wave speed:

$$t_{wave} \sim l_{\parallel}/V_A = l_{\parallel}/c. \quad (74)$$

As in non-relativistic MHD, let us assume critical balance: $t_{eddy} \sim t_{wave}$. Note that, if $t_{eddy} \sim t_{wave}$, an eddy becomes completely distorted after one collision and, therefore, one collision is enough for energy cascade. From Equations (73) and (74), the condition for critical balance, hence for strong relativistic force-free MHD turbulence, becomes

$$\frac{l_{\perp}}{b_l} \sim \frac{l_{\parallel}}{B_0}, \quad (75)$$

which is identical to the one for non-relativistic MHD, if the latter is expressed in terms of b_l rather than v_l . If turbulence driving is isotropic, the condition for critical balance at the driving scale is

$$B_0 \approx b_L \sim b_{rms}, \quad (76)$$

which is also the same as its non-relativistic counterpart.

6.2 Scaling relations in strong relativistic Alfvénic turbulence

By combining constancy of energy cascade rate and critical balance, we can derive energy spectrum and anisotropy for strong relativistic force-free Alfvénic turbulence:

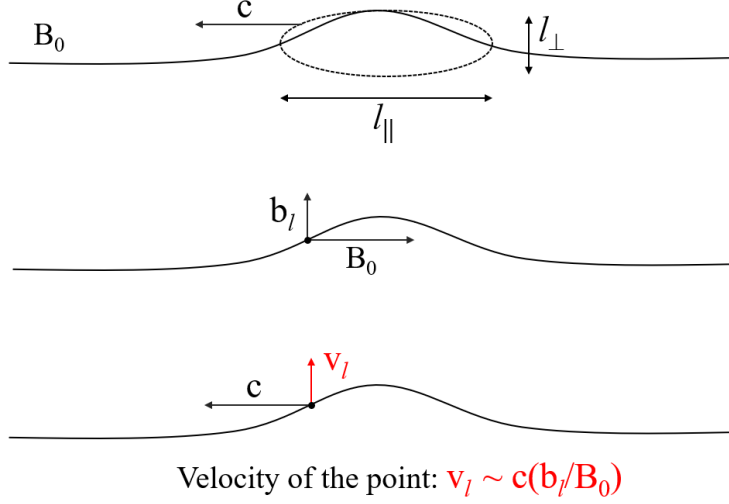


Fig. 10 Propagation of an Alfvénic wave packet. (Upper) An Alfvénic wave packet on scale l moves to the left at the speed of light. (Middle) Typical ‘inclination’ of a magnetic field line on scale l is of order $\sim b_l/B_0$. (Lower) Typical (perpendicular) speed of a point on the magnetic field line due to propagation of the wave packet, is $\sim cb_l/B_0$.

- Constancy of energy cascade rate:

$$b_l^2/t_{cas} = \text{constant}, \quad (77)$$

- Critical balance (i.e., $t_{eddy} = t_{wave}$):

$$\frac{l_{\perp} B_0}{c b_l} \approx \frac{l_{\parallel}}{c}. \quad (78)$$

We can see that these two equations are identical to those for non-relativistic MHD. Therefore, we can conclude that strong relativistic force-free MHD turbulence has Kolmogorov magnetic spectrum

$$E_b(k) \propto k^{-5/3}. \quad (79)$$

and the GS95 anisotropy

$$l_{\parallel} \propto l_{\perp}^{2/3}. \quad (80)$$

In summary, we use constancy of energy cascade rate and critical balance to derive scaling relations in strong relativistic force-free MHD turbulence. The results show that magnetic spectrum and anisotropy are virtually identical to those of strong non-relativistic Alfvénic turbulence.

6.3 Numerical tests

Using a numerical simulation, [Cho \(2005\)](#) confirmed that the scaling relations in the previous subsection, which were first proposed by [Thompson and Blaes \(1998\)](#), hold true. We solved the following system of equations to simulate decaying relativistic force-free Alfvénic turbulence:

$$\frac{\partial \mathbf{Q}}{\partial t} + \frac{\partial \mathbf{F}}{\partial x^1} = 0, \quad (81)$$

where

$$\mathbf{Q} = (S_1, S_2, S_3, B_2, B_3), \quad (82)$$

$$\mathbf{F} = (T_{11}, T_{12}, T_{13}, -E_3, E_2), \quad (83)$$

$$T_{ij} = -(E_i E_j + B_i B_j) + \frac{\delta_{ij}}{2} (E^2 + B^2), \quad (84)$$

$$\mathbf{S} = \mathbf{E} \times \mathbf{B}, \quad (85)$$

$$\mathbf{E} = -\frac{1}{B^2} \mathbf{S} \times \mathbf{B}. \quad (86)$$

Here, \mathbf{E} is the electric field, \mathbf{S} the Poynting flux vector and $c = 1$. (see [Komissarov 2002](#)). Greek indices run from 1 to 4. At $t = 0$ and also at later times for which we calculated energy spectra and anisotropy, the condition for critical balance is satisfied.

The left panel of [Figure 11](#) shows energy spectra of the magnetic field. At $t = 0$ (not shown in the figure) only large-scale (i.e., small k) Fourier modes are excited. At later times, turbulence develops as energy cascades down to small-scale (i.e., large k) modes. After $t \sim 3$, the energy spectrum decreases without changing its slope. The spectrum at this stage is very close to a Kolmogorov spectrum:

$$E_b(k) \propto k^{-5/3}. \quad (87)$$

The right panel of [Figure 11](#) displays that anisotropy of eddy shapes follows the relation

$$l_{\parallel} \propto l_{\perp}^{2/3}. \quad (88)$$

These results are consistent with the theoretical prediction by [Thompson and Blaes \(1998\)](#). [Cho and Lazarian \(2014b\)](#) showed that driven strong relativistic force-free MHD turbulence also follows the same scaling relations.

7 MHD Turbulence in compressible medium

Compressible turbulence is a long-standing problem. Since it is very difficult to analytically study scaling relations of compressible turbulence, many researchers rely on numerical simulations. Nevertheless, there have been quests for scaling relations. Some studies considered weak compressibility. For example, [Zank and Matthaeus \(1993\)](#) studied weakly compressible MHD turbulence and [Lithwick and Goldreich \(2001\)](#) proposed theoretical predictions for compressible turbulence in strongly-magnetized high- β plasmas, in which gas pressure is larger than magnetic pressure and effect

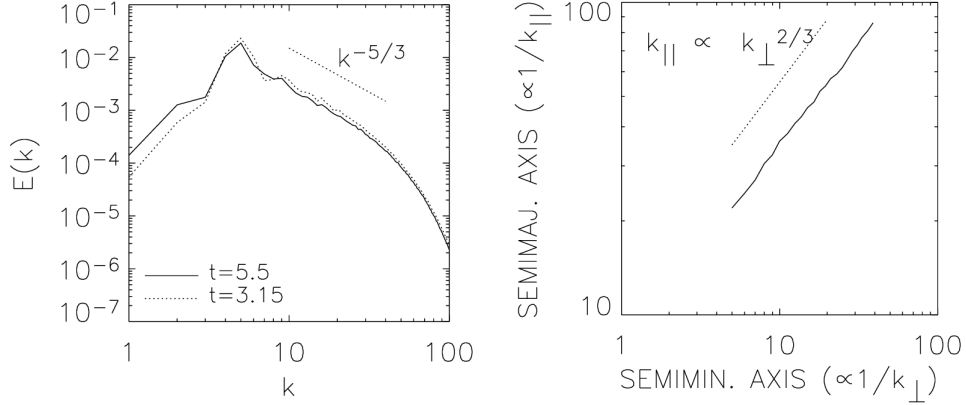


Fig. 11 Scaling relations in strong relativistic force-free MHD turbulence. (Left) Spectrum. (Right) Anisotropy. These scaling relations are virtually identical to those of non-relativistic strong MHD turbulence (i.e., the GS95 scaling relations). From Cho (2005).

of compressibility is marginal. The latter authors claimed that Alfvén modes follow the GS95 scaling relations and cascade of Alfvén modes makes slow modes passively follow the same scaling. There are also studies that considered high compressibility. For example, Cho and Lazarian (2002, 2003) studied scaling relations in supersonic MHD turbulence. On the other hand, Kritsuk et al. (2007) studied energy cascade in supersonic hydrodynamic turbulence. In this section, we briefly introduce the work by Cho and Lazarian (2002, 2003), in which we studied ‘strong’ MHD turbulence in highly compressible medium. Some studies on weak MHD turbulence can be found in Chandran (2008b); Beattie et al. (2020); Lazarian et al. (2025).

7.1 Mode separation method

Three types of waves exist (Alfvén, slow and fast) in a compressible magnetized plasma. Cho and Lazarian (2002, 2003) developed a method to separate different MHD modes and studied their scaling relations. Figure 12 explains the separation method. Here we focus on only velocity separation. The slow, fast, and Alfvén bases that denote the direction of displacement vectors for each mode are given by

$$\hat{\xi}_s \propto (-1 + \alpha - \sqrt{D})k_{\parallel}\hat{\mathbf{k}}_{\parallel} + (1 + \alpha - \sqrt{D})k_{\perp}\hat{\mathbf{k}}_{\perp}, \quad (89)$$

$$\hat{\xi}_f \propto (-1 + \alpha + \sqrt{D})k_{\parallel}\hat{\mathbf{k}}_{\parallel} + (1 + \alpha + \sqrt{D})k_{\perp}\hat{\mathbf{k}}_{\perp}, \quad (90)$$

$$\hat{\xi}_A = -\hat{\varphi} = \hat{\mathbf{k}}_{\perp} \times \hat{\mathbf{k}}_{\parallel}, \quad (91)$$

where $D = (1 + \alpha)^2 - 4\alpha \cos^2 \theta$, $\alpha = a^2/V_A^2 = \beta(\gamma/2)$, θ is the angle between \mathbf{k} and \mathbf{B}_0 , and $\hat{\varphi}$ is the azimuthal basis in the spherical polar coordinate system. (Note that $\gamma = 1$ for isothermal case.) These bases are mutually orthogonal.

In order to separate modes, we perform a simulation of MHD turbulence and obtain a 3-dimensional velocity data cube. Then we compute velocity Fourier components via

the Fourier transform. We obtain Alfvén, slow, and fast Fourier velocity components by projecting the velocity Fourier component $\mathbf{v}_{\mathbf{k}}$ onto $\hat{\xi}_A$, $\hat{\xi}_s$, and $\hat{\xi}_f$, respectively.

7.2 Scaling relations

Figure 13 show the results for a supersonic low- β plasma, where magnetic pressure is larger than gas pressure. The average sonic Mach number is ~ 2.3 and critical balance is satisfied. Upper panels display energy spectra of Alfvén, slow, and fast modes. As we can see, spectra of Alfvén and slow modes follow a Kolmogorov spectrum, while that of fast modes looks shallower than a Kolmogorov spectrum. Lower panels illustrate eddy shapes. Shapes of Alfvén- and slow-mode eddies are scale-dependent: smaller eddies are more elongated. Detailed calculations confirm that they follow the GS95 anisotropy. On the other hand, fast-mode eddies do not show scale-dependent anisotropy. Turbulence in high- β plasmas also exhibit similar scaling relations. Sonic Mach number also does not affect the scaling relations much. In summary, [Cho and Lazarian \(2002, 2003\)](#) found that Alfvén and slow modes follow the GS95 scaling relations.

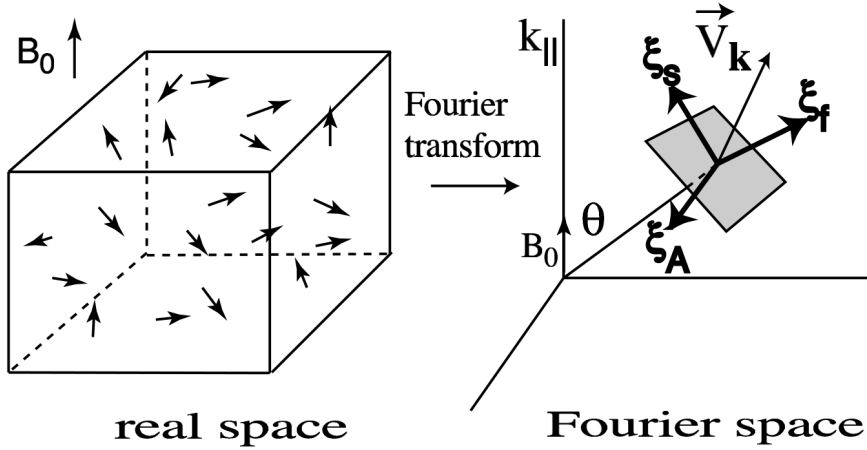


Fig. 12 Separation method. We separate Alfvén, slow, and fast modes in Fourier space by projecting the velocity Fourier component $\mathbf{v}_{\mathbf{k}}$ onto bases ξ_A , ξ_s , and ξ_f , respectively. From [Cho and Lazarian \(2003\)](#).

8 Conclusion

In this paper, we have reviewed the scaling relations of MHD turbulence threaded by a strong mean magnetic field. We have shown that collision of opposite-traveling wave packets is essential for generation of turbulence in various environments. Based on critical balance, which states that one collision is enough to complete energy cascade, we have discussed following scaling relations:

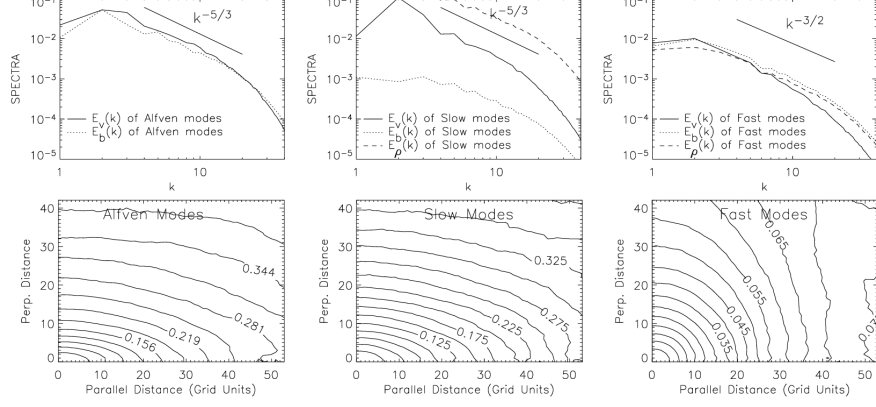


Fig. 13 Scaling relations of Alfvén (left panels), slow (middle panels), and fast (right panels) modes in a low β plasma ($\beta \sim 0.2$, $M_A \sim 0.7$, and $M_s \sim 2.3$). (Upper panels) From left to right, spectra for Alfvén, slow, and fast modes. Spectra of Alfvén and slow modes follow a Kolmogorov-like power law. Spectra for fast modes are shallower. (Lower panels) From left to right, anisotropy for Alfvén, slow, and fast modes. Contours show the second-order structure function of velocity and represent eddy shapes. Alfvén and slow modes follow anisotropy similar to that of GS95 ($l_{\parallel} \propto l_{\perp}^{2/3}$ or $k_{\parallel} \propto k_{\perp}^{2/3}$). Fast modes does not show anisotropy. From [Cho and Lazarian \(2003\)](#).

- strong incompressible Alfvénic MHD turbulence (Section 3):

$$E(k) \propto k^{-5/3} \text{ and } l_{\parallel} \propto k_{\perp}^{2/3}, \quad (92)$$

- strong EMHD turbulence below the proton gyro-scale (Section 5):

$$E(k) \propto k^{-7/3} \text{ and } l_{\parallel} \propto k_{\perp}^{1/3}, \quad (93)$$

- strong relativistic Alfvénic MHD turbulence (Section 6):

$$E(k) \propto k^{-5/3} \text{ and } l_{\parallel} \propto k_{\perp}^{2/3}. \quad (94)$$

Alfvén waves or variants of Alfvén waves play key roles in these types of turbulence. Note that whistler waves, which are important for EMHD turbulence, can be regarded as small-scale version of Alfvén waves, although the dispersion relation for the former is very different from that for the latter.

Turbulence that satisfies critical balance is called strong turbulence. We have shown that Alfvén modes in strong compressible MHD turbulence exhibit the following

scaling relations (Section 7):

$$E(k) \propto k^{-5/3} \text{ and } l_{\parallel} \propto k^{2/3}. \quad (95)$$

We have also discussed scaling relations in weak incompressible MHD turbulence (Section 4):

$$E(k) \propto k^{-2} \text{ and } l_{\parallel} = \text{constant}. \quad (96)$$

Note that weak turbulence becomes strong turbulence on scales below $\sim M_A^2 L$, where L is the energy injection scale and M_A is the Alfvén Mach number.

Conflict of interest

The author declares no conflict of interest.

References

- Batchelor, G.K.: On the Spontaneous Magnetic Field in a Conducting Liquid in Turbulent Motion. *Proceedings of the Royal Society of London Series A* **201**(1066), 405–416 (1950) <https://doi.org/10.1098/rspa.1950.0069>
- Beattie, J.R., Bhattacharjee, A.: Scale-dependent alignment in compressible magnetohydrodynamic turbulence. *arXiv e-prints*, 2504–15538 (2025) <https://doi.org/10.48550/arXiv.2504.15538> [arXiv:2504.15538](https://arxiv.org/abs/2504.15538) [physics.plasm-ph]
- Bruno, R., Carbone, V.: The Solar Wind as a Turbulence Laboratory. *Living Reviews in Solar Physics* **10**(1), 2 (2013) <https://doi.org/10.12942/lrsp-2013-2>
- Beresnyak, A.: MHD turbulence. *Living Reviews in Computational Astrophysics* **5**(1), 2 (2019) <https://doi.org/10.1007/s41115-019-0005-8> [arXiv:1910.03585](https://arxiv.org/abs/1910.03585) [astro-ph.GA]
- Beattie, J.R., Federrath, C., Seta, A.: Magnetic field fluctuations in anisotropic, supersonic turbulence. *Monthly Notices of the Royal Astronomical Society* **498**(2), 1593–1608 (2020) <https://doi.org/10.1093/mnras/staa2257> [arXiv:2007.13937](https://arxiv.org/abs/2007.13937) [astro-ph.GA]
- Beresnyak, A., Lazarian, A.: Polarization intermittency and its influence on mhd turbulence. *The Astrophysical Journal* **640**(2), 175 (2006) <https://doi.org/10.1086/503708>
- Beresnyak, A., Lazarian, A.: Strong Imbalanced Turbulence. *Astrophysical Journal* **682**(2), 1070–1075 (2008) <https://doi.org/10.1086/589428> [arXiv:0709.0554](https://arxiv.org/abs/0709.0554) [astro-ph]

- Beresnyak, A., Lazarian, A.: Comparison of Spectral Slopes of Magnetohydrodynamic and Hydrodynamic Turbulence and Measurements of Alignment Effects. *Astrophysical Journal* **702**(2), 1190–1198 (2009) <https://doi.org/10.1088/0004-637X/702/2/1190> [arXiv:0812.0812](https://arxiv.org/abs/0812.0812) [astro-ph]
- Boldyrev, S.: On the spectrum of magnetohydrodynamic turbulence. *The Astrophysical Journal* **626**(1), 37 (2005) <https://doi.org/10.1086/431649>
- Boldyrev, S.: Spectrum of magnetohydrodynamic turbulence. *Phys. Rev. Lett.* **96**, 115002 (2006) <https://doi.org/10.1103/PhysRevLett.96.115002>
- Biskamp, D., Schwarz, E., Drake, J.F.: Two-Dimensional Electron Magnetohydrodynamic Turbulence. *Phys. Rev. Lett.* **76**(8), 1264–1267 (1996) <https://doi.org/10.1103/PhysRevLett.76.1264>
- Brandenburg, A., Sokoloff, D., Subramanian, K.: Current Status of Turbulent Dynamo Theory. From Large-Scale to Small-Scale Dynamos. *Space Science Reviews* **169**(1-4), 123–157 (2012) <https://doi.org/10.1007/s11214-012-9909-x> [arXiv:1203.6195](https://arxiv.org/abs/1203.6195) [astro-ph.SR]
- Biskamp, D., Schwarz, E., Zeiler, A., Celani, A., Drake, J.F.: Electron magnetohydrodynamic turbulence. *Physics of Plasmas* **6**(3), 751–758 (1999) <https://doi.org/10.1063/1.873312>
- Blandford, R.D., Znajek, R.L.: Electromagnetic extraction of energy from Kerr black holes. *Monthly Notices of the Royal Astronomical Society* **179**, 433–456 (1977) <https://doi.org/10.1093/mnras/179.3.433>
- Chandran, B.D.G.: Strong Anisotropic MHD Turbulence with Cross Helicity. *Astrophysical Journal* **685**(1), 646–658 (2008) <https://doi.org/10.1086/589432> [arXiv:0801.4903](https://arxiv.org/abs/0801.4903) [astro-ph]
- Chandran, B.D.G.: Weakly Turbulent Magnetohydrodynamic Waves in Compressible Low- β Plasmas. *Physical Review Letters* **101**(23), 235004 (2008) <https://doi.org/10.1103/PhysRevLett.101.235004> [arXiv:0810.5360](https://arxiv.org/abs/0810.5360) [astro-ph]
- Chen, C.H.K.: Recent progress in astrophysical plasma turbulence from solar wind observations. *Journal of Plasma Physics* **82**(6), 535820602 (2016) <https://doi.org/10.1017/S0022377816001124> [arXiv:1611.03386](https://arxiv.org/abs/1611.03386) [physics.plasm-ph]
- Cho, J.: Simulations of Relativistic Force-free Magnetohydrodynamic Turbulence. *Astrophysical Journal* **621**(1), 324–327 (2005) <https://doi.org/10.1086/427493> [arXiv:astro-ph/0408318](https://arxiv.org/abs/astro-ph/0408318) [astro-ph]
- Cho, J.: Magnetic Helicity Conservation and Inverse Energy Cascade in Electron Magnetohydrodynamic Wave Packets. *Phys. Rev. Lett.* **106**(19), 191104 (2011) <https://doi.org/10.1103/PhysRevLett.106.191104> [arXiv:1104.4148](https://arxiv.org/abs/1104.4148) [astro-ph.EP]

- Cho, J.: Origin of Magnetic Field in the Intracluster Medium: Primordial or Astrophysical? *Astrophysical Journal* **797**(2), 133 (2014) <https://doi.org/10.1088/0004-637X/797/2/133> arXiv:1410.1893 [astro-ph.CO]
- Cho, J., Lazarian, A.: Compressible Sub-Alfvénic MHD Turbulence in Low- β Plasmas. *Physical Review Lett.* **88**(24), 245001 (2002) <https://doi.org/10.1103/PhysRevLett.88.245001> arXiv:astro-ph/0205282 [astro-ph]
- Cho, J., Lazarian, A.: Compressible magnetohydrodynamic turbulence: mode coupling, scaling relations, anisotropy, viscosity-damped regime and astrophysical implications. *Monthly Notices of the Royal Astronomical Soc.* **345**(12), 325–339 (2003) <https://doi.org/10.1046/j.1365-8711.2003.06941.x> arXiv:astro-ph/0301062 [astro-ph]
- Cho, J., Lazarian, A.: The Anisotropy of Electron Magnetohydrodynamic Turbulence. *Astrophysical Journal Lett.* **615**(1), 41–44 (2004) <https://doi.org/10.1086/425215> arXiv:astro-ph/0406595 [astro-ph]
- Cho, J., Lazarian, A.: Simulations of Electron Magnetohydrodynamic Turbulence. *Astrophysical Journal* **701**(1), 236–252 (2009) <https://doi.org/10.1088/0004-637X/701/1/236> arXiv:0904.0661 [astro-ph.EP]
- Cho, J., Lazarian, A.: Imbalanced Relativistic Force-free Magnetohydrodynamic Turbulence. *Astrophysical Journal* **780**(1), 30 (2014) <https://doi.org/10.1088/0004-637X/780/1/30> arXiv:1312.6128 [astro-ph.HE]
- Cho, J., Lazarian, A.: Imbalanced Relativistic Force-free Magnetohydrodynamic Turbulence. *Astrophysical Journal* **780**(1), 30 (2014) <https://doi.org/10.1088/0004-637X/780/1/30> arXiv:1312.6128 [astro-ph.HE]
- Cho, J., Lazarian, A., Vishniac, E.T.: Simulations of magnetohydrodynamic turbulence in a strongly magnetized medium. *The Astrophysical Journal* **564**(1), 291 (2002) <https://doi.org/10.1086/324186>
- Cho, J., Vishniac, E.T.: The Anisotropy of Magnetohydrodynamic Alfvénic Turbulence. *Astrophysical Journal* **539**(1), 273–282 (2000) <https://doi.org/10.1086/309213> arXiv:astro-ph/0003403 [astro-ph]
- Cho, J., Vishniac, E.T.: The Generation of Magnetic Fields through Driven Turbulence. *Astrophysical Journal* **538**(1), 217–225 (2000) <https://doi.org/10.1086/309127> arXiv:astro-ph/0003404 [astro-ph]
- Cho, J., Vishniac, E.T., Beresnyak, A., Lazarian, A., Ryu, D.: Growth of magnetic fields induced by turbulent motions. *The Astrophysical Journal* **693**(2), 1449 (2009) <https://doi.org/10.1088/0004-637X/693/2/1449>

- Dmitruk, P., Matthaeus, W.H.: Structure of the electromagnetic field in three-dimensional Hall magnetohydrodynamic turbulence. *Physics of Plasmas* **13**(4), 042307 (2006) <https://doi.org/10.1063/1.2192757>
- Duncan, R.C., Thompson, C.: Formation of Very Strongly Magnetized Neutron Stars: Implications for Gamma-Ray Bursts. *Astrophysical Journal* **392**, 9 (1992) <https://doi.org/10.1086/186413>
- Dastgeer, S., Zank, G.P.: Anisotropic Turbulence in Two-dimensional Electron Magnetohydrodynamics. *Astrophysical Journal* **599**(1), 715–722 (2003) <https://doi.org/10.1086/379225>
- Frisch, U.: *Turbulence: The Legacy of A. N. Kolmogorov*. Cambridge University Press, ??? (1995)
- Galtier, S.: Wave turbulence in incompressible Hall magnetohydrodynamics. *Journal of Plasma Physics* **72**(5), 721–769 (2006) <https://doi.org/10.1017/S0022377806004521> [arXiv:physics/0608227](https://arxiv.org/abs/physics/0608227) [physics.space-ph]
- Galtier, S., Bhattacharjee, A.: Anisotropic weak whistler wave turbulence in electron magnetohydrodynamics. *Physics of Plasmas* **10**(8), 3065–3076 (2003) <https://doi.org/10.1063/1.1584433>
- Galtier, S., Bhattacharjee, A.: Anisotropic wave turbulence in electron mhd. *Plasma Physics and Controlled Fusion* **47**(12B), 691 (2005) <https://doi.org/10.1088/0741-3335/47/12B/S51>
- Goldreich, P., Julian, W.H.: Pulsar Electrodynamics. *Astrophysical Journal* **157**, 869 (1969) <https://doi.org/10.1086/150119>
- Galtier, S., Nazarenko, S.V., Newell, A.C., Pouquet, A.: A weak turbulence theory for incompressible magnetohydrodynamics. *Journal of Plasma Physics* **63**(5), 447–488 (2000) <https://doi.org/10.1017/S0022377899008284> [arXiv:astro-ph/0008148](https://arxiv.org/abs/astro-ph/0008148) [astro-ph]
- Goldreich, P., Sridhar, S.: Toward a Theory of Interstellar Turbulence. II. Strong Alfvénic Turbulence. *Astrophysical Journal* **438**, 763 (1995) <https://doi.org/10.1086/175121>
- Goldreich, P., Sridhar, S.: Magnetohydrodynamic Turbulence Revisited. *Astrophysical Journal* **485**(2), 680–688 (1997) <https://doi.org/10.1086/304442> [arXiv:astro-ph/9612243](https://arxiv.org/abs/astro-ph/9612243) [astro-ph]
- Howes, G.G., Cowley, S.C., Dorland, W., Hammett, G.W., Quataert, E., Schekochihin, A.A., Tatsuno, T.: Howes et al. Reply:. *Phys. Rev. Lett.* **101**(14), 149502 (2008) <https://doi.org/10.1103/PhysRevLett.101.149502> [arXiv:0812.2493](https://arxiv.org/abs/0812.2493) [astro-ph]

- Howes, G.G., Dorland, W., Cowley, S.C., Hammett, G.W., Quataert, E., Schekochihin, A.A., Tatsuno, T.: Kinetic Simulations of Magnetized Turbulence in Astrophysical Plasmas. *Phys. Rev. Lett.* **100**(6), 065004 (2008) <https://doi.org/10.1103/PhysRevLett.100.065004> [arXiv:0711.4355](https://arxiv.org/abs/0711.4355) [astro-ph]
- Horbury, T.S., Forman, M., Oughton, S.: Anisotropic scaling of magnetohydrodynamic turbulence. *Phys. Rev. Lett.* **101**, 175005 (2008) <https://doi.org/10.1103/PhysRevLett.101.175005>
- Iroshnikov, P.S.: Turbulence of a Conducting Fluid in a Strong Magnetic Field. *Soviet Astronomy* **7**, 566 (1964)
- Kazantsev, A.P.: Enhancement of a Magnetic Field by a Conducting Fluid. *Soviet Journal of Experimental and Theoretical Physics* **26**, 1031 (1968)
- Kim, H., Cho, J.: Inverse Cascade in Imbalanced Electron Magnetohydrodynamic Turbulence. *Astrophysical Journal* **801**(2), 75 (2015) <https://doi.org/10.1088/0004-637X/801/2/75>
- Kingsep, A., Chukbar, K., Yankov, V., Kadomtsev, B.: Reviews of plasma physics. Consultant bureau, New York **16** (1990)
- Kritsuk, A.G., Norman, M.L., Padoan, P., Wagner, R.: The Statistics of Supersonic Isothermal Turbulence. *Astrophysical Journal* **665**(1), 416–431 (2007) <https://doi.org/10.1086/519443> [arXiv:0704.3851](https://arxiv.org/abs/0704.3851) [astro-ph]
- Kolmogorov, A.N.: The local structure of turbulence in incompressible viscous fluid for very large reynolds. Numbers. In *Dokl. Akad. Nauk SSSR* **30**, 301 (1941)
- Kolmogorov, A.N.: A refinement of previous hypotheses concerning the local structure of turbulence in a viscous incompressible fluid at high reynolds number. *Journal of Fluid Mechanics* **13**(1), 82–85 (1962) <https://doi.org/10.1017/S0022112062000518>
- Komissarov, S.S.: Time-dependent, force-free, degenerate electrodynamics. *Monthly Notices of the Royal Astronomical Society* **336**(3), 759–766 (2002) <https://doi.org/10.1046/j.1365-8711.2002.05313.x> [arXiv:astro-ph/0202447](https://arxiv.org/abs/astro-ph/0202447) [astro-ph]
- Kraichnan, R.H.: Inertial-range spectrum of hydromagnetic turbulence. *The Physics of Fluids* **8**(7), 1385–1387 (1965) <https://doi.org/10.1063/1.1761412> https://pubs.aip.org/aip/pfl/article-pdf/8/7/1385/12617184/1385.1_online.pdf
- Kida, S., Yanase, S., Mizushima, J.: Statistical properties of mhd turbulence and turbulent dynamo. *Physics of Fluids A: Fluid Dynamics* **3**(3), 457–465 (1991) <https://doi.org/10.1063/1.858102> https://pubs.aip.org/aip/pof/article-pdf/3/3/457/12402462/457.1_online.pdf
- Lytikov, M., Blandford, R.: Gamma Ray Bursts as Electromagnetic Outflows.

- arXiv e-prints, 0312347 (2003) <https://doi.org/10.48550/arXiv.astro-ph/0312347> [arXiv:astro-ph/0312347](https://arxiv.org/abs/0312347) [astro-ph]
- Lithwick, Y., Goldreich, P.: Compressible Magnetohydrodynamic Turbulence in Interstellar Plasmas. *Astrophysical Journal* **562**(1), 279–296 (2001) <https://doi.org/10.1086/323470> [arXiv:astro-ph/0106425](https://arxiv.org/abs/0106425) [astro-ph]
- Lithwick, Y., Goldreich, P., Sridhar, S.: Imbalanced Strong MHD Turbulence. *Astrophysical Journal* **655**(1), 269–274 (2007) <https://doi.org/10.1086/509884> [arXiv:astro-ph/0607243](https://arxiv.org/abs/0607243) [astro-ph]
- Lazarian, A., Ho, K.W., Yuen, K.H., Vishniac, E.: Sub-Alfvénic Turbulence: Magnetic-to-kinetic Energy Ratio, Modification of Weak Cascade, and Implications for Magnetic Field Strength Measurements. *Astrophysical Journal* **978**(1), 88 (2025) <https://doi.org/10.3847/1538-4357/ad8d49> [arXiv:2312.05399](https://arxiv.org/abs/2312.05399) [astro-ph.GA]
- Leamon, R.J., Smith, C.W., Ness, N.F., Matthaeus, W.H., Wong, H.K.: Observational constraints on the dynamics of the interplanetary magnetic field dissipation range. *Journal of Geophysical Research: Space Physics* **103**(A3), 4775–4787 (1998) <https://doi.org/10.1029/97JA03394> <https://agupubs.onlinelibrary.wiley.com/doi/pdf/10.1029/97JA03394>
- Leamon, R.J., Smith, C.W., Ness, N.F., Wong, H.K.: Dissipation range dynamics: Kinetic Alfvén waves and the importance of β_e . *Journal of Geophysical Research* **104**(A10), 22331–22344 (1999) <https://doi.org/10.1029/1999JA900158>
- Meneguzzi, M., Frisch, U., Pouquet, A.: Helical and nonhelical turbulent dynamos. *Phys. Rev. Lett.* **47**, 1060–1064 (1981) <https://doi.org/10.1103/PhysRevLett.47.1060>
- Maron, J., Goldreich, P.: Simulations of Incompressible Magnetohydrodynamic Turbulence. *Astrophysical Journal* **554**(2), 1175–1196 (2001) <https://doi.org/10.1086/321413> [arXiv:astro-ph/0012491](https://arxiv.org/abs/0012491) [astro-ph]
- Meyrand, R., Galtier, S., Kiyani, K.H.: Direct evidence of the transition from weak to strong magnetohydrodynamic turbulence. *Phys. Rev. Lett.* **116**, 105002 (2016) <https://doi.org/10.1103/PhysRevLett.116.105002>
- Montgomery, D., Matthaeus, W.H.: Anisotropic Modal Energy Transfer in Interstellar Turbulence. *Astrophysical Journal* **447**, 706 (1995) <https://doi.org/10.1086/175910>
- Matthaeus, W.H., Oughton, S., Ghosh, S., Hossain, M.: Scaling of anisotropy in hydro-magnetic turbulence. *Phys. Rev. Lett.* **81**, 2056–2059 (1998) <https://doi.org/10.1103/PhysRevLett.81.2056>
- Mason, J., Perez, J.C., Boldyrev, S., Cattaneo, F.: Numerical simulations of strong incompressible magnetohydrodynamic turbulence. *Physics of Plasmas*

- 19**(5), 055902–055902 (2012) <https://doi.org/10.1063/1.3694123> arXiv:1202.3474 [physics.plasm-ph]
- Matthaeus, W.H., Servidio, S., Dmitruk, P.: Comment on “Kinetic Simulations of Magnetized Turbulence in Astrophysical Plasmas”. *Phys. Rev. Lett.* **101**(14), 149501 (2008) <https://doi.org/10.1103/PhysRevLett.101.149501>
- Montgomery, D., Turner, L.: Anisotropic magnetohydrodynamic turbulence in a strong external magnetic field. *The Physics of Fluids* **24**(5), 825–831 (1981) <https://doi.org/10.1063/1.863455> https://pubs.aip.org/aip/pfl/article-pdf/24/5/825/12722146/825_1_online.pdf
- Ng, C.S., Bhattacharjee, A.: Scaling of anisotropic spectra due to the weak interaction of shear-Alfvén wave packets. *Physics of Plasmas* **4**(3), 605–610 (1997) <https://doi.org/10.1063/1.872158>
- Ng, C.S., Bhattacharjee, A., Germaschewski, K., Galtier, S.: Anisotropic fluid turbulence in the interstellar medium and solar wind. *Physics of Plasmas* **10**(5), 1954–1962 (2003) <https://doi.org/10.1063/1.1567291>
- Perez, J.C., Boldyrev, S.: Role of Cross-Helicity in Magnetohydrodynamic Turbulence. *Phys. Rev. Lett.* **102**(2), 025003 (2009) <https://doi.org/10.1103/PhysRevLett.102.025003> arXiv:0807.2635 [astro-ph]
- Podesta, J.J., Bhattacharjee, A.: Theory of Incompressible Magnetohydrodynamic Turbulence with Scale-dependent Alignment and Cross-helicity. *Astrophysical Journal* **718**(2), 1151–1157 (2010) <https://doi.org/10.1088/0004-637X/718/2/1151> arXiv:0903.5041 [astro-ph.EP]
- Perez, J.C., Mason, J., Boldyrev, S., Cattaneo, F.: On the Energy Spectrum of Strong Magnetohydrodynamic Turbulence. *Physical Review X* **2**(4), 041005 (2012) <https://doi.org/10.1103/PhysRevX.2.041005> arXiv:1209.2011 [astro-ph.SR]
- Podesta, J.J.: Dependence of solar-wind power spectra on the direction of the local mean magnetic field. *The Astrophysical Journal* **698**(2), 986 (2009) <https://doi.org/10.1088/0004-637X/698/2/986>
- Schekochihin, A.A., Cowley, S.C., Dorland, W., Hammett, G.W., Howes, G.G., Quataert, E., Tatsuno, T.: Astrophysical Gyrokinetics: Kinetic and Fluid Turbulent Cascades in Magnetized Weakly Collisional Plasmas. *Astrophysical Journal Supp.* **182**(1), 310–377 (2009) <https://doi.org/10.1088/0067-0049/182/1/310> arXiv:0704.0044 [astro-ph]
- Schekochihin, A.A.: MHD turbulence: a biased review. *Journal of Plasma Physics* **88**(5), 155880501 (2022) <https://doi.org/10.1017/S0022377822000721> arXiv:2010.00699 [physics.plasm-ph]

- Schekochihin, A.A., Cowley, S.C., Taylor, S.F., Maron, J.L., McWilliams, J.C.: Simulations of the small-scale turbulent dynamo. *The Astrophysical Journal* **612**(1), 276 (2004) <https://doi.org/10.1086/422547>
- Sridhar, S., Goldreich, P.: Toward a Theory of Interstellar Turbulence. I. Weak Alfvénic Turbulence. *Astrophysical Journal* **432**, 612 (1994) <https://doi.org/10.1086/174600>
- Saito, S., Gary, S.P., Li, H., Narita, Y.: Whistler turbulence: Particle-in-cell simulations. *Physics of Plasmas* **15**(10), 102305 (2008) <https://doi.org/10.1063/1.2997339>
- Smith, C.W., Hamilton, K., Vasquez, B.J., Leamon, R.J.: Dependence of the Dissipation Range Spectrum of Interplanetary Magnetic Fluctuations on the Rate of Energy Cascade. *Astrophysical Journal Lett.* **645**(1), 85–88 (2006) <https://doi.org/10.1086/506151>
- Shebalin, J.V., Matthaeus, W.H., Montgomery, D.: Anisotropy in mhd turbulence due to a mean magnetic field. *Journal of Plasma Physics* **29**(3), 525–547 (1983) <https://doi.org/10.1017/S0022377800000933>
- Thompson, C., Blaes, O.: Magnetohydrodynamics in the extreme relativistic limit. *Physical Review D* **57**(6), 3219–3234 (1998) <https://doi.org/10.1103/PhysRevD.57.3219>
- Thompson, C.: A model of gamma-ray bursts. *Monthly Notices of the Royal Astronomical Society* **270**, 480–498 (1994) <https://doi.org/10.1093/mnras/270.3.480>
- Wicks, R.T., Horbury, T.S., Chen, C.H.K., Schekochihin, A.A.: Power and spectral index anisotropy of the entire inertial range of turbulence in the fast solar wind. *Monthly Notices of the Royal Astronomical Society: Letters* **407**(1), 31–35 (2010) <https://doi.org/10.1111/j.1745-3933.2010.00898.x> https://academic.oup.com/mnrasl/article-pdf/407/1/L31/56932461/mnrasl_407_1_L31.pdf
- Zakharov, V.E., L’Vov, V.S., Falkovich, G.: *Kolmogorov Spectra of Turbulence I: Wave Turbulence*, (1992)
- Zank, G.P., Matthaeus, W.H.: Nearly incompressible fluids. II: Magnetohydrodynamics, turbulence, and waves. *Physics of Fluids A* **5**(1), 257–273 (1993) <https://doi.org/10.1063/1.858780>
- Zhao, S., Yan, H., Liu, T.Z., Yuen, K.H., Wang, H.: Identification of the weak-to-strong transition in Alfvénic turbulence from space plasma. *Nature Astronomy* **8**, 725–731 (2024) <https://doi.org/10.1038/s41550-024-02249-0> [arXiv:2301.06709](https://arxiv.org/abs/2301.06709) [astro-ph.SR]